Desalination and Water Treatment 16 (2010) 110–119
www.deswater.com April

1944-3994/1944-3986 © 2010 Desalination Publications. All rights reserved
doi: 10.5004/dwt.2010.1087

Performance evaluation of nanofiltration membranes for diafiltration of dye/salt mixtures: experimental observations and model verification

Jiří Cuhorka, Petr Mikulášek*

University of Pardubice, Faculty of Chemical Technology, Institute of Environmental and Chemical Engineering, Studentská 573, Pardubice 532 10, Czech Republic
Tel. +420 466 037 503; Fax: +420 466 037 068; email: petr.mikulasek@upce.cz

Received 16 April 2009; Accepted 13 December 2009

ABSTRACT

The process of desalination of aqueous dye-salt solutions by polymeric nanofiltration membranes using commercially available modules were studied.

The experimental part was focused on determination of basic characteristics of tested membranes (Esna 1, Desal 5DK, NF 70, NF 90, NF 270 and TR 60), which above all, means determination of the dependence of permeate flow intensity or rejection on pressure difference used. The demineralised water and water solution of NaCl are used to characterize all of the tested membranes.

Great interest is also attached to the mathematical modelling of nanofiltration and description of discontinuous diafiltration by periodically adding solvent at constant pressure difference.

Keywords: Nanofiltration; Diafiltration; Reactive dyes; Dye desalination

1. Introduction

In dye manufacture, like most other processes, there is continual search for production methods that will improve product yield and reduce manufacturing costs. Dye desalting and purification, the process by which impurities are removed to improve the quality of the product, is currently one of the biggest applications for nanofiltration (NF) technology. Dye manufacturers are now actively pursuing desalting of the finished dye prior to spray drying because it not only improves product quality, but makes spray drying more efficient because the granulation of the dye takes place without the production dust. NF is proving to be an ideal method for this salt removal [1,2].

Nanofiltration is the most recently developed pressure-driven membrane separation process and has properties that lie between those of ultrafiltration (UF) and reverse osmosis (RO). The nominal molecular weight cut-off (MWCO) of NF membranes is in the range of 200–1000 Da. Separation may be due to solution diffusion, sieving effects, Donnan and dielectric effects. The rejection is low for salts with mono-valent anion and non-ionized organics with a molecular weight below 150, but is high for salts with di- and multi-valent anions and organics with a molecular weight above 300. Thus, NF can be used for the simultaneous removal of sodium chloride (salt) and the concentration of aqueous dye solutions [3,4].

Diafiltration is the process of washing dissolved species through the membrane, which is to improve the recovery of the material in permeate, or to enhance the purity of the retained stream. Typical applications can be found in the recovery of biochemical products from their fermentation broths. Furthermore, diafiltration can be found in removal of free hydrogel present in external solution to purify of a semi-solid liposome (SSL), purification of polymer nanoparticles, enhancing the protein

---

*Corresponding author.

lactose ratio in whey protein products, separating sugars or dye from NaCl solution (desalting), and many other fields. According to the property of the solute and the selectivity of membrane, diafiltration can be used in the process of MF, UF or NF [5–9,13].

Great interest is also attached to the mathematical modelling of nanofiltration and description of discontinuous diafiltration by periodically adding solvent at constant pressure difference. This diafiltration consists of two processes: concentration and dilute mode. In the concentration mode retentate stream is recirculated to the feed tank and the permeate stream is collected separately. No diluant is added in this mode. Diluant is added in the second operation process. These two processes are one diafiltration step.

The proposed mathematical model connects the design equations and model of permeation through the membrane. The transport through the membrane depends on the different approaches. Firstly, the membrane is regarded to a dense layer and in this case transport is based on solution–diffusion model [10,11]. Second approach of membrane is regarded to porous medium. Models with this approach are based mainly on extended Nerns–Planck equation. By this approach, a system containing any number of n ions can be described using set of $(3n + 2)$ equations. In this approach, it is assumed that the flux of every ion through the membrane is induced by pressure, concentration and electrical potentials. These models describe the transport of ions in terms of an effective pore radius r_p (m), an effective membrane thickness/porosity ratio $\Delta x/A_k$ (m) and an effective membrane charge density X_d (mol/m^{-3}). Such a model requires many experiments for determination of these structural parameters. These models are hard to solve [4,9,12,13]. The last approach is based on irreversible thermodynamics. These models assume the membrane as "black box" and have been applied in predicting transport through NF membranes for binary systems (Kedem–Katchalsky, Spiegler–Kedem models). Perry and Linder extended the Spiegler and Kedem model to describe the salt rejection in the presence of organic ion. This model describes transport of ion through membrane in terms of salt permeability P_s, reflection coefficient σ [7,13–15]. In our work the solution–diffusion model is used. We propose an easy way to describe concentration in feed for batch operations. The solution–diffusion model can be replaced by a more theoretical model in future.

Before diafiltration experiments, characterizations of membranes are made. Water and salt solutions were used for these characterizations. From the results, suitable membranes for desalination were chosen—Desal 5DK, NF 70, NF 270 and TR 60.

2. Mathematical modelling

Mathematical model connects together balance equations and solution–diffusion model, which is extended by dependence of salt permeability on the salt concentration in feed and Donnan equilibrium.

The balances for the concentration mode can be written as:

Solvent mass balance:

$$\frac{d\left(V_F\rho_F\right)}{d\tau} = -\ JA^*\rho_P \tag{1}$$

Mass balances of dye and salt:

$$\frac{d\left(V_F c_{D,F}\right)}{d\tau} = -\ \ JA^* c_{D,P} \tag{2}$$

$$\frac{d\left(V_F c_{S,F}\right)}{d\tau} = -\ JA^* c_{S,P} \tag{3}$$

Eq. (1) can be written as:

$$\frac{dV_F}{d\tau} = -J_V A^* \tag{4}$$

Mass balances of dye and salt are formally same and we can solve them together. Subscripts i represent dye and salt. Eq. (2) (or (3)), may be re-written as:

$$\frac{d\left(V_F c_{i,F}\right)}{d\tau} = -J_V A^* \left(1 - R_i\right) c_{i,F} \tag{5}$$

where R_i is real rejection.

In the concentration mode, the volume and the concentration in feed depends on the time. Expanded differential equation with using the product rule can be written as:

$$V_F \frac{dc_{i,F}}{d\tau} + c_{i,F}\frac{dV_F}{d\tau} = -J_V A^* \left(1 - R_i\right) c_{i,F} \tag{6}$$

Substituting Eq. (4) into Eq. (6) leads to:

$$V_F \frac{dc_{i,F}}{d\tau} = J_V A^* R_i c_{i,F} \tag{7}$$

Dividing Eq. (7) by Eq. (4) leads to:

$$V_F \frac{dc_{i,F}}{dV_F} = -R_i c_{i,F} \tag{8}$$

If we assume constant rejection and permeate flux (for small change of volume in feed tank, or better of yield–permeate volume divided by feed volume, it is achieved) or the average value integrations of Eq. (8) and Eq. (4) with the boundary conditions (V_{F0} to V_F) resulting in Eq. (9) and Eq. (10):

$$c_{i,F} = c_{i,F0}\left(\frac{V_{F0}}{V_F}\right)^{R_i} \tag{9}$$

$$\tau = \frac{V_{R0} - V_R}{J_V A^*} \tag{10}$$

On the base of Eqs. (9) and (10) we can obtain the concentration in feed tank and the time for separation of certain permeate volume in concentration mode, respectively.

The next process is diluting using pure solvent (water) as diluant. Salt concentration in feed tank after this operation (c_S') is:

$$c_S' = c_{i,F0}\left(\frac{V_F}{V_{F0}}\right) \tag{11}$$

This concentration (c_S') is now equal to the salt concentration in feed tank ($c_{S,F0}$) for the next concentration mode in the second diafiltration step.

For solving these equations we need to know the dependence of rejection and permeate flux on salt concentration in feed.

The basic equations for rejection can be written as:

$$J_S = B\left(c_F - c_P\right) \tag{12}$$

$$c_P = \frac{J_S}{J_V} \tag{13}$$

This model can be extended by the dependence of salt permeability on salt concentration in the feed [15]. To avoid some inconveniences with units, here c^* is introduced and chosen to be 1 g/l.

$$B = \alpha.\left(\frac{c_{S,F}}{c^*}\right)^{\beta} \tag{14}$$

Assuming equilibrium on the membrane–solution interface we can obtain (approximating activities with concentrations) [15]:

$$c_{S,W} = c_{S,F}.\left(1 + \frac{\nu_D . c_{D,F} . M_S}{c_{S,F} . M_D}\right) \tag{15}$$

In the presence of Donnan exclusion forces, induced by the impermeable organic ions, the salt transport across the membrane proceeds as if the membrane was exposed to a salt solution having concentration $c_{S,W}$ instead of $c_{S,F}$. Thus the value of $c_{S,W}$ and not that of $c_{S,F}$ determines the driving force for the passage of salt.

The expression for salt passage in the presence of retained organic ion can be written as:

$$J_S = \alpha\left(\frac{c_{S,F}}{c^*}\right)^{\beta}\left(c_{S,W} - c_{S,P}\right) \tag{16}$$

and salt concentration in permeate can be expressed as

$$c_{S,P} = \frac{\alpha\,\frac{c_{S,F}^{\beta+1}}{c^{*\beta}}\left(1 + \frac{\nu_D . c_{D,F} . M_S}{c_{S,F} . M_D}\right)}{J_V + \alpha\, c_{S,F}^{\beta} c^{*-\beta}} \tag{17}$$

For the permeate flux these equations can be use:

$$J_V = A\left(\Delta P - \Delta\pi_s - \delta\right) \tag{18}$$

Eq. (18) is the osmotic pressure model. This model is used in similar form by many authors [3,7,10–11,13–15]. Parameter A (water permeability) can be concentration or viscous dependent [10,13]. For our model we assume this parameter as constant. Coefficient δ represents the effect of dye on flux. This means mainly osmotic pressure of dye. If this parameter represents only osmotic pressure of dye, then it is constant too (constant dye concentration).

The osmotic pressure gradient for salt is related to the difference of the concentration Δc by the van´t Hoff's law:

$$\Delta\pi_S = \frac{\nu R^* T}{M}\Delta c_S \tag{19}$$

where c is concentration.

3. Characterization of membrane

Before diafiltration experiments, characterizations of commercial membranes are carried out. For these characterizations pure water and water solutions of salt are used. From experiments with pure water model, parameter A (water permeability) can be estimated. This parameter is slope of the curve (straight line) $J = f\,(\Delta P)$ (see Eq. 18 and $\Delta\pi = \delta = 0$ because no salt and dye are used). In our model we assume water permeability as constant. However, an increase in concentration can cause significant changes in viscosity and a consequent modification of the water permeability. According to resistance model ($A = 1/(\mu R_M)$) the dependence of water permeability on viscosity can be expresed as:

$$A_\mu = \frac{A}{\mu_{REL}} \tag{20}$$

where A is the water permeability with respect to pure water and μ_{REL} is the relative viscosity of feed solution to pure water [13].

In case of diafiltration, fouling or gel layer effects can occur and then parameter A is dependent on dye/salt concentration ratio (in resistance model is added next resistance $A = 1/\mu_{REL}\,(R_M + R_F)$, where R_M and R_F are membrane and fouling resistance [10]).

Similar experiments are made with salt solutions. Four salt concentrations (1, 5, 10 and 35 g/l) are used. From these experiments we obtain parameter B (salt permeability) and then α and β plotting B versus c_F). Values obtained from these experiments are not used direct but are used as first approximation values for best fit parameters (see Table 3). From results (salt rejection and flux) the suitable membranes for desalination were chosen—Desal 5DK, NF 70, NF 270 and TR 60. Membranes NF 90 and Esna 1 had higher rejection (see Fig. 3). For desalination membranes with small rejection of salt are suitable.

4. Comparison of membranes

For comparison of membranes, three factors were used:

The first factor is separation factor of diafltration, S:

$$S = \frac{\frac{c_D}{c_D^0}}{\frac{c_S}{c_S^0}} = \frac{c_D c_S^0}{c_D^0 c_S} \tag{21}$$

where c_D^0, c_S^0 are concentrations of dye and salt at the beginning of the experiment, c_D, c_S are concentrations of dye and salt at the end of experiment.

The separation factor, S, represents how well the dye will be desalinated. With higher separation factor the dye desalination is better. But it is also clear that with bigger separation factor the loss of the dye will be bigger because real membranes do not have 100% rejection of dye.

The dye loss factor, Z, can be defined as the rate of amount of the dye in permeate to amount of the dye at the beginning of experiment:

$$Z = \frac{V.\left(c_D^0 - c_D\right)}{V.c_D^0} = 1 - \frac{c_D}{c_D^0} \tag{22}$$

The third parameter is time of diafiltration needed to reach certain separation factor, S. The total time of diafiltration with n steps, τ can be expressed (constant permeate flux in each concentraion mode) as:

$$\tau_{total} = \sum_{i=1}^{n} \frac{\Delta V}{Q} = \sum_{i=1}^{n} \frac{V_{F0} - V_F}{A\,.\,J} \tag{23}$$

where Q is flow of permeate.

5. Experimental

5.1. Membranes

Six NF membranes were chosen for this study. All membranes are made from polyamide and their membrane area was 3 m^2. The MWCO can be seen in [16–18], except NF 70, data for this membrane is not available. Properties of membranes used are given in Table 1.

5.2. Materials

Dye was obtained from VÚOS a.s. Pardubice. The commercial name (in Czech) is: Ostazinová žlut' H-R 33 TEK, and a molecular weight is 674.05 in free acid form (three acidic groups) or 740.02 as the sodium salt. Fig. 1 shows structural formula of the free acid form.

NaCl used for all experiments was analytical grade. The demineralised water with the conductivity between 4-15 μS/cm was used in this study.

5.3. Methods

Dye concentrations were analysed using a spectrophotometer (SPECOL 11). NaCl concentrations were determined from conductivity measurements using a conductivity meter (Cond 340i). Permeate and retentate salt concentrations during diafiltrations experiments were analysed using potentiometric titration.

5.4. Experimental system

The experiments were carried out on system depicted schematically in Fig. 2. Feed (F) was pumped by pump (3) (Wanner Engineering, Inc., type Hydracell G13) from feed vessel (2) to membrane module (1). Pressure was set by valve (4) placed behind membrane module. Permeate (P) and retentate (R) were brought back to feed vessel. Pressure was measured by manometer (5). Temperature was detected by thermometer (6). Stable temperature was maintained by cooling system (7). Temperature in all experiments was 23°C.

5.5. Filtration procedure

The system was operated in the full recirculation mode while both retentate and permeate were continuously recirculated to the feed tank except sampling and concentration mode of diafiltration. By changing applied pressure (from 5 to 30 bar) and concentration of salt (1, 5, 10 and 35 g/l) in characterization of membranes both the retentate and permeate were returned back to the feed tank for 10 min or 0.5 h, respectively to reach a steady state before sampling. Before first concentration mode in diafiltraton experiments and after each diluting mode the total recirculation was used 1 h and minimally 5 min, respectively. The permeate flux was measured by weighing of certain permeate volume and using a stopwatch.

Table 1
Properties of the membranes.

Indication	Type	Producer	MWCO [Da]	Material	Module
Desal 5DK	Desal 5DK	GEW PT	200	polyamide	spiral-wound
Esna 1	Esna 1	Hydranautics	100-300	polyamide	spiral-wound
NF 90	NF 90	Dow	90	polyamide	spiral-wound
NF 270	NF 270	Dow	270	polyamide	spiral-wound
NF 70	CSM NE 2540 - 70	Saehan	-	polyamide	spiral-wound
TR 60	TR 60 - 2540	Toray	400	polyamide	spiral-wound

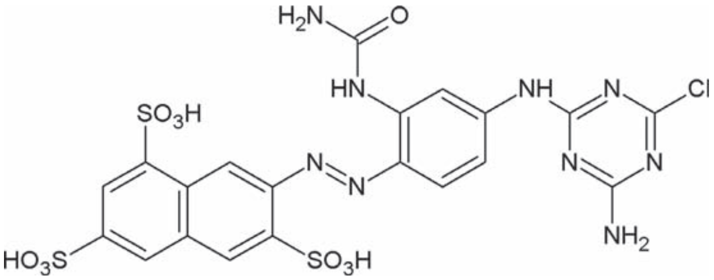

Fig. 1. Structural formula of dye (free acid) used.

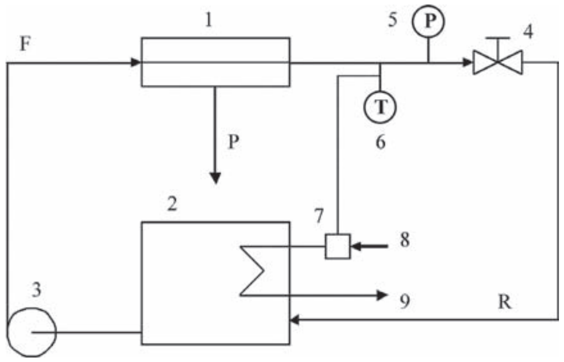

Fig. 2. Schematic diagram of the experimental set-up used. 1 membrane module, 2 feed vessel, 3 high pressure pump, 4 back pressure valve, 5 manometer, 6 temperature controller, 7 cooling system, 8 cooling water input, 9 cooling water output, F feed, P permeate, R retentate (concentrate).

6. Results and discussion

6.1. Pure water flux

Water permeability is one of the basic characteristic of NF membranes. According to Darcy's law, the permeate flux is directly proportional to the pressure difference across the membrane. The slope of this line corresponds to the water permeability (A).

6.2. Rejection of NaCl

Basic membrane characteristics are the dependence of the permeate flux and salt rejection on other operation parameters, i.e. the applied pressure difference and the salt concentration in feed.

The permeate flux increases with increasing pressure and decreases as the feed concentration of salt increases. For the lowest concentration of salt (1 g/l), the values of permeate flux were similar to the values of clean water. The lower values of permeate flux were obtained with increasing salt concentrations in feed (increasing osmotic pressure). For membrane NF 90 measured fluxes were at the highest salt concentration for pressure smaller than 25 bar, because the osmotic pressure was too high. The opposite was the problem with membrane NF 270 at the smallest salt concentration in feed. The permeate flux was too high and pump was not able to deliver necessary volumetric flow of retentate (600 l/h) for constant conditions at all experiments.

The observed rejection increases as the pressure difference increases, and decreases with the increasing salt concentration in feed for all tested membranes. However, minimal values were obtained during experiments with membrane NF 270. Low values of salt rejection and higher values of permeate flux are suitable for desalting. Fig. 3 shows the comparison of tested membranes for the lowest and highest salt concentrations in feed (35 g/l), respectively.

6.3. Diafiltration

Batch diafiltration with periodically adding solvent at 20 bars and constant retentate flow 600 l/h was provided. Aqueous dye solutions with dye concentrations 100, 50 and 10 g/l and salt concentration between 20–23 g/l were desalted at 23°C. Volume of the pure solvent added in every dilute mode was 4 l (The same volume of permeate was removed before in concentration mode). Total feed volume in tank was 52 l. For every membrane and every concentration of the dye in feed, fifty diafiltration steps were made. One point in Figs. 4–7 is one diafiltration step before concentration mode.

Table 2
Water permeability of membranes used.

Membrane	A [l/m^2.h.bar]
Desal 5DK	3,365
Esna 1	4,824
NF 90	5,845
NF 270	6,801
NF 70	2,650
TR 60	3,952

Only four membranes—Desal 5DK, NF 70, NF 270 and TR 60 were used for diafiltration experiments. Diafiltration with membrane NF 270 was provided only with dye concentrations 100 and 50–g/l and with membrane TR 60 only at the highest dye concentration, which is the best for desalination. For the reason of low values of permeate flux, membrane NF 90 and Esna 1 were not used for those experiments.

Dependences of rejection on salt concentration in feed are given in Fig. 4 for Desal 5DK, NF 70, NF 270 and TR 60, respectively. Membranes are compared at dye concentration 100–g/l. The lowest values of rejection (max. 0.29) were obtained for membrane Desal 5DK. The membrane NF 70 had the highest values.

Dependences of flux on salt concentrations are shown in Fig. 5. The highest values of flux (70.3 l/m^2.h) were obtained in experiments with membrane NF 270. Fig. 6 shows the dependences of salt concentrations on time of diafiltration.

The comparisons of experimental and model data for the highest dye concentration (100 g/l) are shown in Fig. 7. Salt concentrations are calculated using Eq. (9) and Eq. (11). Rejection needed for these equations is calculated on basis of Eq. (17). Best fit parameters for proposed model are given in Table 3.

From Table 3 it can be shown that δ is not only osmotic pressure (if we assume water permeability as constant), because the values of δ are different. From these results we can assume, the highest effect of dye

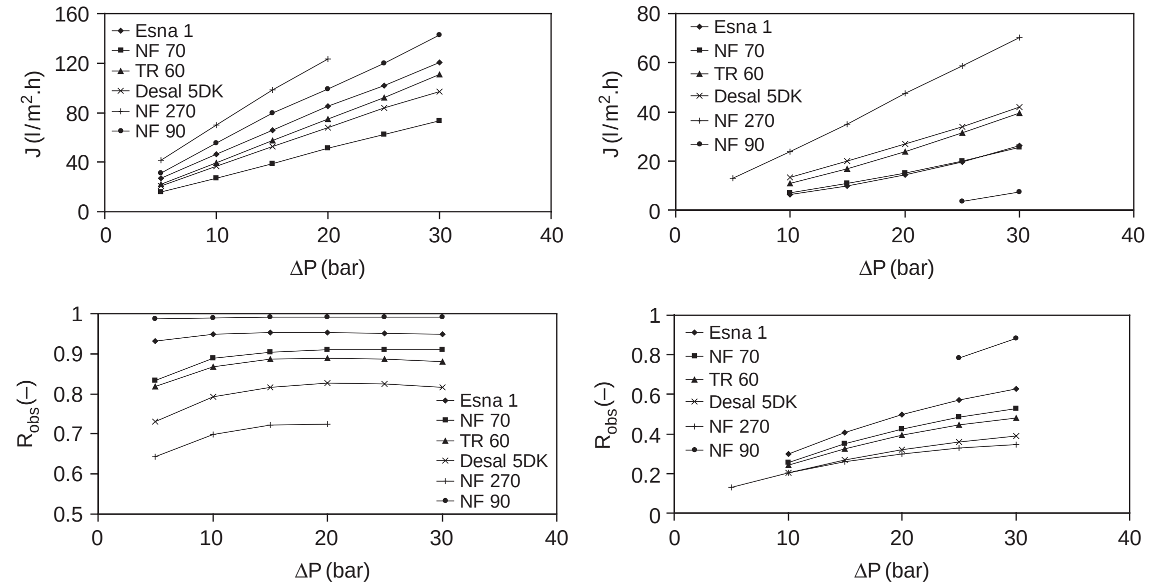

Fig. 3. Permeate flux and rejection as a function of pressure for the lowest salt concentration (1 g/l) - figures on left and the highest salt concentration (35 g/l) – figures on right.

on flux is for membrane NF 270. This membrane is the most fouled from these membranes. It is appropriate to assume that there is change in water permeability (A) in case of desalination of dyes.

Table 4 clearly shows, that the total time of diafiltration τ decreases with decreasing dye concentration. The membrane NF 270 had the shortest time. Time for the highest dye concentration is not two times higher than with medium dye concentration for all tested membranes (the time/amount of dye desalted ratio is smaller for higher concentration of dye). Separation factor decreases with decreasing concentration of dye and it is the second reason why the highest dye concentration was used as the best mode for desalination. Membrane Desal 5DK had the best separation factor (membrane NF 270 had very similar values, except the highest dye

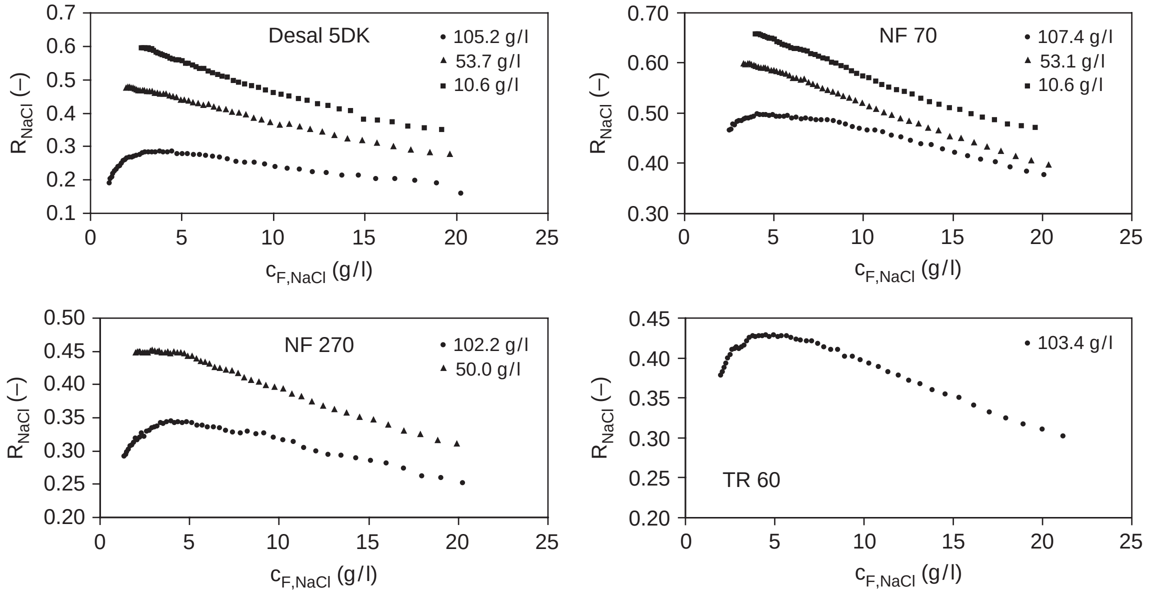

Fig. 4. Salt rejection as a function of salt concentration in feed.

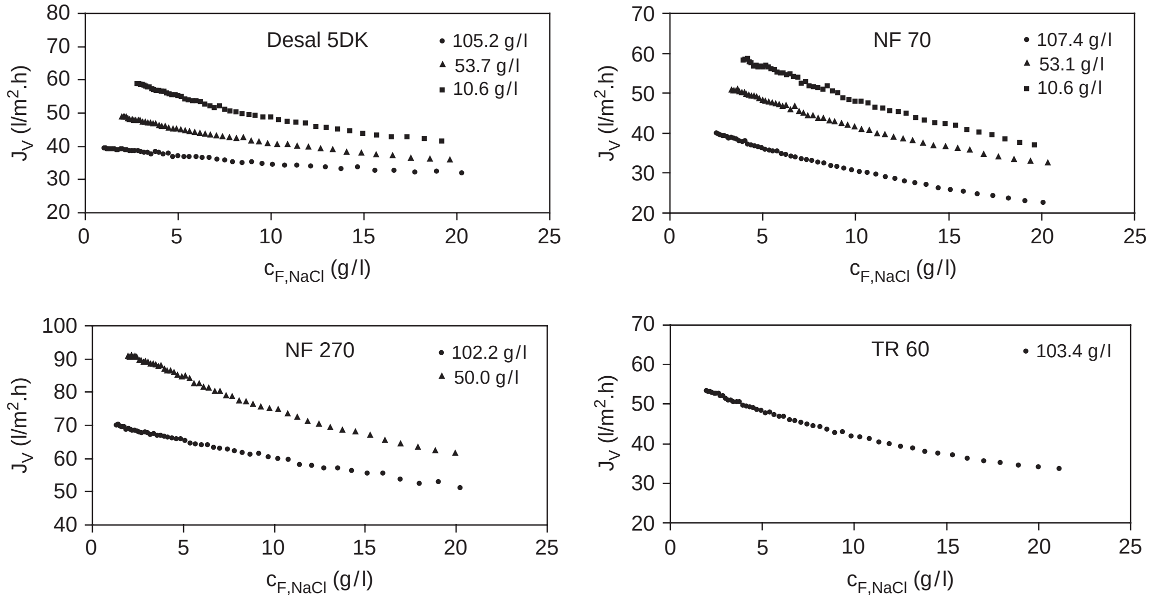

Fig. 5. Permeate flux as a function of salt concentration in feed.

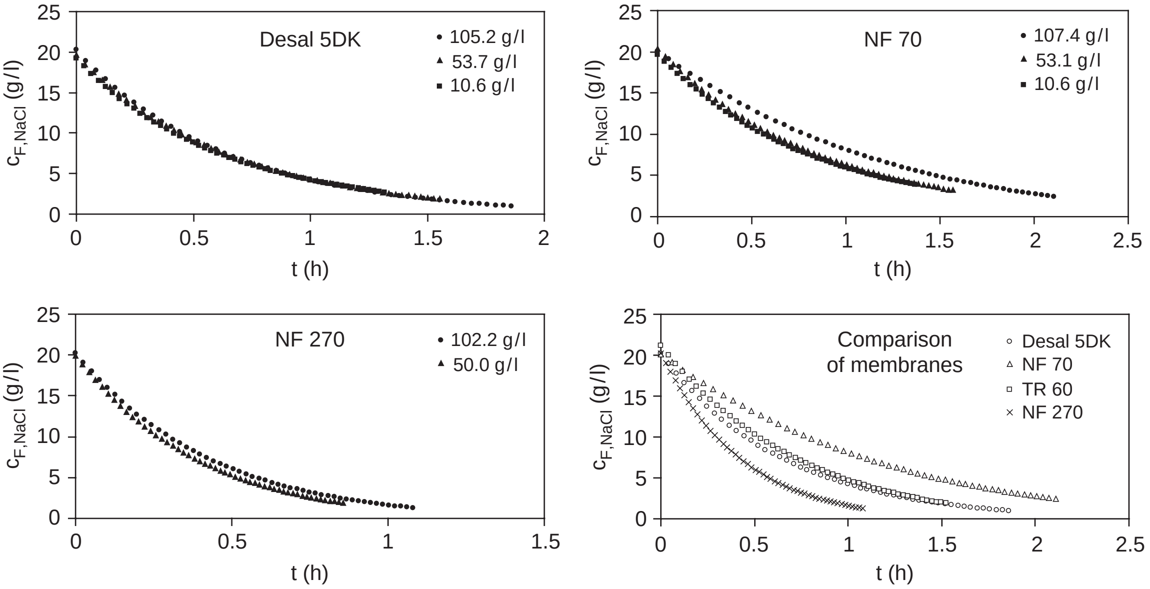

Fig. 6. Salt concentration as a function of diafiltration time for membranes Desal 5DK, NF 70, NF 270 and comparison of tested membranes at dye concentration 100 g/l.

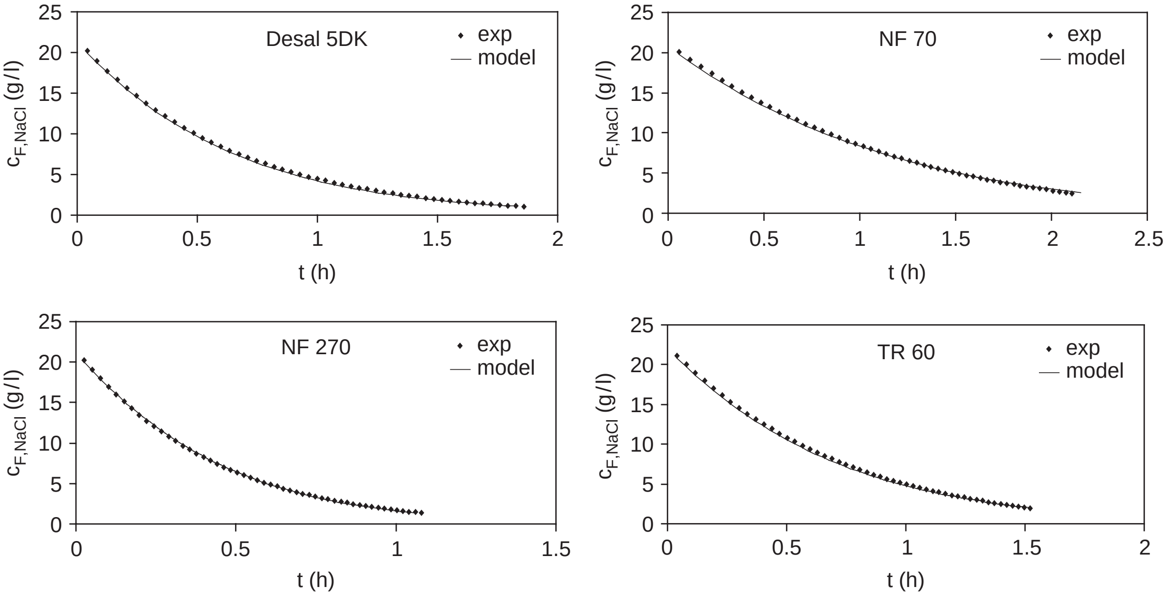

Fig. 7. Comparison of experimental and model data for the highest dye concentration.

Table 3
Model parameters.

Membrane	A [l/m2.h.bar]	α[l/m2.h]	β[-]	δ[bar]
Desal 5DK	3.365	5.758	0.620	7.503
NF 70	2.650	4.839	0.381	4.664
NF 270	6.800	10.350	0.529	8.561
TR 60	3.952	6.693	0.474	5.888

concentration). The loss of dye is almost same for membrane Desal 5DK, NF 70 and NF 270 at all concentrations of dye. Only for membrane TR 60 are obtained higher loss of dye.

7. Conclusions

From the results presented above it is clear that the best concentration of the dye in feed for desalination of

Table 4
Total time of diafiltration, τ total, the separation factor, S, and the loss of dye, Z. (Subscripts Z, K are start and end of diafiltration).

		DESAL 5DK		
c_F,NaCl,Z	(g/l)	22.00	19.62	19.21
c_F,NaCl,K	(g/l)	0.97	1.88	2.70
c_F,dye,Z	(g/l)	105.17	53.75	10.61
c_F, dye,K	(g/l)	105.15	53.74	10.60
τ_{total}	(hod)	1.86	1.55	1.32
S	(-)	22.71	10.44	7.10
Z	(%)	0.02	0.01	0.07
		NF 70		
c_F,NaCl,Z	(g/l)	20.08	20.33	19.64
c_F,NaCl,K	(g/l)	2.40	3.21	3.86
c_F, dye,Z	(g/l)	107.42	53.05	10.56
c_F, dye,K	(g/l)	107.38	53.04	10.56
τ_{total}	(hod)	2.11	1.57	1.37
S	(-)	8.37	6.34	5.09
Z	(%)	0.03	0.03	0.05
		TR 60		
c_F,NaCl,Z	(g/l)	21.14	20.56	19.72
c_F,NaCl,K	(g/l)	1.88	2.22	3.16
c_F, dye,Z	(g/l)	103.41	53.65	10.71
c_F, dye,K	(g/l)	102.74	53.16	10.52
τ_{total}	(hod)	1.52	1.25	0.98
S	(-)	11.17	8.98	6.25
Z	(%)	0.65	0.48	0.18
		NF 270		
c_F,NaCl,Z	(g/l)	22.00	19.92	20.64
c_F,NaCl,K	(g/l)	1.28	1.90	2.68
c_F, dye,Z	(g/l)	102.15	49.98	10.52
c_F, dye,K	(g/l)	102.12	49.97	10.53
τ_{total}	(hod)	1.08	0.86	0.67
S	(-)	17.19	10.50	6.89
Z	(%)	0.03	0.04	0.04

reactive dye by batch diafiltration is 100 g/l. In this case the salt rejection reaches minimal value due to Donnan potential which strengthens the flow of salt through the membrane.

The best membrane for desalination is NF 270 which has smaller dye loss factor and the shortest time of diafiltration. Very suitable membrane is also Desal 5DK, which has the best separation factor and dye loss factor, but this membrane has longer time of diafiltration (see Table 4). For desalination qualitative description it is convenient to use the proposed model.

Acknowledgments

This project was financially supported by Ministry of Education, Youth and Sports of the Czech Republic, Project MSM0021627502.

Nomenclature

A^*	membrane area
A	water permeability
B	salt permeability
J	flux
M	relative molecular mass
R	rejection
R^*	universal gas constant

Greeks

α	coefficient for salt permeability,
β	coefficient for concentration dependence of salt permeability
δ	coefficient for dye solution,
σ	reflection coefficient
ν	valence (for NaCl is $\nu = 2$ and for dye $\nu = 3$).

Subscripts

0	- beginning of the concentration mode
D	- dye
F	- feed
P	- permeate
R	- retentate
S	- salt
V	- water
W	- membrane interface (wall)

References

[1] S. Yu, C. Gao, H. Su and M. Liu, Nanofiltration used for desalination and concentration in dye production, Desalination, 140 (2001) 9–100.

[2] Y. He, G.M. Li, J.F. Zhao and H.X. Su, Membrane technology: Reactive dyes and cleaner production, Filtration & Separation, 44 (2007) 22–23.

[3] M. Mulder, Basic Principles of Membrane Technology, 2nd Ed., Kluwer Academic Publisher, 2000.

[4] D.L. Oatley, B. Cassey, P. Jones and W.R. Bowen, Modelling the performance of membrane nanofiltration – recovery of high-value product from a process waste stream, Chem. Eng. Sci., 60 (2005) 1953–1964.

[5] G. Foley, Water usage in variable volume diafiltration: comparison with ultrafiltration and constant volume diafiltration, Desalination, 196 (2006) 160–163.

[6] K. Weselowska, S. Koter and M. Bodzek, Modelling of nanofiltration in softening water, Desalination, 163 (2004) 137–151.

[7] H. Al-Zoubi, N. Hilal, N.A. Darwish and A.W. Mohammed, Rejection and modelling of sulphate and potassium salts by nanofiltration membranes: neural network and Spiegler-Kedem model, Desalination, 206 (2007) 42–60.

[8] L. Wang, G. Yang, W. Xing and N. Xu, Mathematic model of yield for diafiltration, Sep. Purif. Technol., 59 (2008) 206–213.

[9] W.R. Bowen and A.W. Mohammad, Diafiltration by Nanofiltration: Prediction and Optimization, AIChE J., 44 (1998) 1799–1812.

[10] E. Cséfalvay, V. Pauer and P. Mizsey, Recovery of copper from process waters by nanofiltration and reverse osmosis, Desalination, 240 (2009) 132–146.

[11] Ch. Das, S. Dasgupta and S. De, Steady-state modeling for membrane separation of pretreated soaking effluent under cross flow mode, Environmental Progress, 27 (2008) 346–352.

[12] A.A. Hussain, S.K. Nataraj, M.E.E. Abashar, I.S. Al-Mutaz and T.M. Aminabhavi, Prediction of physical properties of nanofiltration membranes using experiment and theoretical models, J. Membr. Sci., 310 (2008) 321–336.

[13] Z. Kovacs, M. Discacciati and W. Samhaber, Modelling of batch and semi-batch membrane filtration processes, J. Membr. Sci., 327 (2009) 164–173.

[14] Z. Kovács, M. Discacciati and W. Samhaber, Modelling of amino acid nanofiltration by irreversible thermodynamics, J. Membr. Sci., 332 (2009) 38–49.

[15] I. Koyuncu and D. Topacik, Effect of organic ion on the separation of salts by nanofiltration membranes, J. Membr. Sci., 195 (2002) 247–263.

[16] N. Park, B. Kwon, M. Sun, H. Ahn, Ch. Kim, Ch. Kwoak, D. Lee, S. Chae, H. Hyung and J. Cho, Application of various membranes to remove NOM typically occurring in Korea with respect to DBP, AOC and transport, Desalination, 178 (2005) 161–169.

[17] M. Tahaikt, A. Ait Haddou, R. El Habbani , Z. Amor, F.Elhannouni, M. Taky, M. Kharif, A. Boughriba, M. Hafsi and A. Elmidaoui, Comparison of the performances of three commercial membranes in fluoride removal by nanofiltration. Continuous operations, Desalination, 225 (2008) 209–219.

[18] G. Bargeman, J.M. Vollenbroek, J. Straatsma, C.G.P.H. Schroën and R.M. Boom, Nanofiltration of multi-component feeds. Interactions between neutral and charged components and their effect on retention, J. Membr. Sci., 247 (2005) 11–20.